Molecular Crystals and Liquid Crystals
Publication details, including instructions for authors and subscription information:
http://www.tandfonline.com/loi/gmcl16

Structural Characterization and Band Electronic Structure of α-(BEDT-TTF)$_2$I$_3$ below its 135 K Phase Transition

Thomas J. Emge [a], Peter C. W. Leung [a], Mark A. Beno [a], Hau H. Wang [a], Jack M. Williams [a], Myung-Hwan Whangbo [b] & Michel Evain [b c]

[a] Chemistry and Materials Science and Technology Divisions, Argonne National Laboratory, Argonne, IL, 60439

[b] Department of Chemistry, North Carolina State University, Raleigh, NC, 27695

[c] Laboratoire de Chimie des Solides, Universite de Nantes, 44072, Nantes, CEDEX, France

Version of record first published: 17 Oct 2011.

To cite this article: Thomas J. Emge , Peter C. W. Leung , Mark A. Beno , Hau H. Wang , Jack M. Williams , Myung-Hwan Whangbo & Michel Evain (1986): Structural Characterization and Band Electronic Structure of α-(BEDT-TTF)$_2$I$_3$ below its 135 K Phase Transition, Molecular Crystals and Liquid Crystals, 138:1, 393-410

To link to this article: http://dx.doi.org/10.1080/00268948608071772

Mol. Cryst. Liq. Cryst., 1986, Vol. 138, pp. 393–410
0026-8941/86/1384–0393/$20.00/0

Printed in the United States of America

Structural Characterization and Band Electronic Structure of α-(BEDT-TTF)$_2$I$_3$ below its 135 K Phase Transition

THOMAS J. EMGE, PETER C. W. LEUNG, MARK A. BENO, HAU H. WANG and JACK M. WILLIAMS†

Chemistry and Materials Science and Technology Divisions, Argonne National Laboratory, Argonne, IL 60439

and

MYUNG-HWAN WHANGBO† and MICHEL EVAIN‡

Department of Chemistry, North Carolina State University, Raleigh, NC 27695

(*Received December 9, 1985; in final form March 11, 1986*)

The nature of the 135 K metal-insulator (MI) transition in α-(BEDT-TTF)$_2$I$_3$, abbreviated α-(ET)$_2$I$_3$, was examined by determining the crystal structures above (298 K) and below (120 K) the phase transition and also by calculating the band electronic structures at both temperatures. This study demonstrates that both the crystal and band electronic structures of α-(ET)$_2$I$_3$ change only slightly upon passing through the MI transition. Within each sheetlike network of ET radical cations, the magnitudes of interactions between adjacent pairs of ET molecules (i–j) above and below the MI transition temperature (T_{MI}) were evaluated by calculating their interaction energies, $\beta_{ij} = \langle\psi_i|H_{eff}|\psi_j\rangle$, where ψ_i and ψ_j are the HOMO's of ET molecules i and j, respectively. The band electronic structures calculated by using single-zeta Slater type orbitals show that α-(ET)$_2$I$_3$ is a semiconductor with band gaps of 13 meV (298 K) and 35 meV (120 K). Thus, within the one-electron model, the apparently metallic properties of α-(ET)$_2$I$_3$ above T_{MI} originate from this extremely small band gap. The band electronic structures calculated by using double-zeta Slater type orbitals also show that α-(ET)$_2$I$_3$ is a semiconductor at both temperatures, but they do not provide a simple explanation for the MI transition. All valence and conduction bands calculated by using either

†Authors to whom correspondence should be addressed.
‡Present address: Laboratoire de Chimie des Solides, Universite de Nantes, 44072 Nantes, CEDEX, France.

single- or double-zeta basis set are very narrow (each less than 100 meV) and are not separated by large energy gaps. Consequently, the one-electron viewpoint may not be adequate in describing the MI transition of α-$(ET)_2I_3$, and the possibility of electron localization in the ET stacks as a result of either electron-electron (Coulomb) repulsion or mixed valence may then be considered.

INTRODUCTION

Syntheses of the *ambient pressure* organic superconductors based upon bis(ethylenedithio)tetrathiafulvalene (BEDT-TTF or simply ET, **1**), i.e., β-$(ET)_2X$ with $X^- = I_3^-$ ($T_c \sim 1.4$ K),[1-3] $X^- = IBr_2^-$ ($T_c \sim 2.7$ K),[4,5] and $X^- = AuI_2^-$ ($T_c \sim 4.5$ K),[6,7] have been pivotal breakthroughs in recent investigations of new organic metals. These isostructural superconductors are

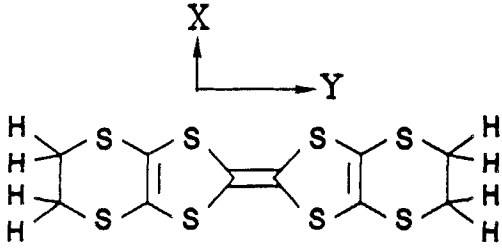

BEDT-TTF or "ET" **1**

two-dimensional (2D) metals,[2,8,9] whose electrical conductivities are nearly the same in magnitude for all directions within the crystallographic *ab* plane. The crystal structures of these β-$(ET)_2X$ salts with I_3^-,[3,10] IBr_2^-,[4,11] and AuI_2^-,[6] are characterized by 2D networks of interacting ET molecules which are made up of identical and parallel stacks of ET molecules in the *ab* plane.

During the electrocrystallization of β-$(ET)_2X$ salts with $X^- = I_3^-$, IBr_2^- and AuI_2^- (which have unit cell volumes[3,4,6,11] of $\sim$800 Å^3 and maximum peak-to-peak ESR linewidths[12] of $\sim$25 gauss at 298 K), other phases, namely α-$(ET)_2X$, which have unit cell volumes[13-15] of $\sim$1600 Å^3 and maximum peak-to-peak ESR linewidths[12] (298 K) of $\sim$90 gauss, are also frequently obtained. Among these α-phase salts, α-$(ET)_2I_3$ has been the subject of several studies concerning its structure[13,16] and physical[17-21] properties. Like β-$(ET)_2I_3$, the crystal structure of α-$(ET)_2I_3$ contains sheetlike networks of ET molecules that are separated by layers of I_3^- anions. However, each 2D ET molecular network within α-$(ET)_2I_3$ has a herringbone arrangement

of the *two* unique ET stacks per unit cell.[13] The electrical conductivity of α-$(ET)_2I_3$ has been described as 2D metallic,[9,17,18] and more anisotropic than that of β-$(ET)_2I_3$.[2,9,17] In contrast to β-$(ET)_2I_3$, which remains metallic[1-3] down to the superconducting onset temperature of 1.4 K, α-$(ET)_2I_3$ undergoes a metal-insulator (MI) transition at ~135 K at ambient pressure.[17,18] This transition is also observed at ~135 K from very recent ESR Studies.[19]

The estimated band electronic structure of α-$(ET)_2I_3$ at room temperature, based upon calculations of HOMO overlap integrals between nearest-neighbor pairs of ET molecules,[20,21] suggested that α-$(ET)_2I_3$ could be either a semi-metal or a semiconductor with a small band gap. It was also noted[22] that the four ET molecules in the complete unit cell have different HOMO energies, so that the possibility of mixed-valence exists in α-$(ET)_2I_3$. Thus, the origin of the metallic properties in α-$(ET)_2I_3$ above its MI transition temperature (T_{MI}) was not clearly understood. So far, the crystal structure of α-$(ET)_2I_3$ below T_{MI} has not been reported. To gain some insight into the nature of the MI transition in α-$(ET)_2I_3$, we have determined its crystal structure at 298 and 120 K and subsequently carried out band electronic structure calculations based upon these structural results above and below T_{MI}.

X-RAY DIFFRACTION RESULTS

Crystals of α-$(ET)_2I_3$ were grown by a previously described electrocrystallization procedure.[3] Unit cell parameters, x-ray data collection details and the results of the least-squares refinement of the crystal structures at 298 K and 120 K are given in Table I. On the basis of x-ray diffraction axial photographs, superlattice intensities were not observed at either temperature. In addition, neutron diffraction data were collected[23] with a large single crystal of α-$(ET)_2I_3$ at 298 K and 20 K, which also showed no indications of superlattice intensities at either temperature. Based on the results of these diffraction experiments, it is likely that the metal-insulator transition of α-$(ET)_2I_3$ at 135 K is not accompanied by a crystallographic transition, and hence the crystal structures at 298 K and 120 K are expected to be very similar except for some shrinkage due to temperature lowering.

The atomic parameters derived from the 298 K and 120 K x-ray data are listed in Table II. Calculated H atom coordinates were located near their observed peaks on the difference-Fourier map. The bond lengths and angles for the ET molecules and I_3^- anions at 298 K

TABLE I

Unit cell data and x-ray data collection parameters and refinement results for α-$(ET)_2I_3$ at 298/120 K

Space group $P\bar{1}$ ($Z = 2$) temperature[a]	298 K	120 K
a (Å)	9.183(1)	9.080(2)
b (Å)	10.804(2)	10.720(3)
c (Å)	17.442(2)	17.390(3)
α (°)	96.96(1)	96.69(2)
β (°)	97.93(1)	97.76(2)
γ (°)	90.85(1)	91.14(2)
V (Å^3)	1698.4(4)	1664.7(6)
d_{calc} (g cm^{-3})	2.25	2.29
T_{min}, T_{max}	0.46, 0.65	0.46, 0.65
μ (mm^{-1})[b]	3.70	3.77
2θ range (°)[c]	0–60	0–60
no. data collected	10700	10604
R_{ave} ($\Sigma\|F_i - \langle F\rangle\|/\Sigma\langle F\rangle$)	0.02	0.02
no. obs. ($F > 0$)	9664	9666
excursions (e^-/Å^3)[d]	±1.5	±2.5
R(F)[e]	0.065	0.054
wR(F)	0.061	0.081
GOF	2.96	5.76

[a] No significant variations of the intensities of the reference reflections were observed throughout both data collections.

[b] Radiation was graphite-monochromatized MoK_α, $\lambda = 0.7107$ Å. The flat hexagon crystal had dimensions of 0.35 × 0.33 × 0.29 × 0.10 mm, along [110], [1–10], [010] and [001], respectively.

[c] The $\theta/2\theta$ scan mode was used, the scan beginning 1.2° below the Mo$K\alpha_1$ and ending 1.3° above the Mo$K\alpha_2$ diffracted beam. All data were LP and absorption corrected.

[d] In both cases, the maximum residuals on the final difference Fourier map were in the vicinity of the I atoms.

[e] $R(F) = [\Sigma||F_{obs}| - |F_{calc}||/\Sigma|F_{obs}|]$;
$wR(F) = [\Sigma w(|F_{obs}| - |F_{calc}|)^2/\Sigma wF_{obs}^2]^{1/2}$;
$GOF = [\Sigma w(|F_{obs}| - |F_{calc}|)^2/(n - m)]^{1/2}$,
for n observations and $m = 355$ variable parameters. The terms $\Sigma w(|F_{obs}| - |F_{calc}|)^2$ were minimized with weights $w = 1/\sigma^2(F_0)$. Atomic scattering factors (with corrections for anomalous dispersion for the I, S, and C atoms) were taken from The International Tables for X-ray Crystallography (1974).

and 120 K are given in Table III. The geometries of the unique ET molecules, labelled A, B and C in Figure 1, at 298 K are nearly identical to those at 120 K and to each other within experimental errors. Also, the ET molecule geometries in α-$(ET)_2I_3$ are nearly the same as to those in the β-$(ET)_2X$ salts with $X^- = I_3^-$, I_2Br^-, IBr_2^- and AuI_2^-, which contain only *one* unique ET molecule per unit cell.[3,4,6,10,11] Thus, within the precision of the x-ray diffraction ex-

TABLE II

Positional and equivalent thermal parameters for α-(ET)$_2$I$_3$ at 298/120 K[a]

Atom	X	Y	Z	U_{eq}
I1	0 / 0	50000 / 50000	50000 / 50000	389(3)/149(2)
I2	30670(2)/30976(4)	57150(2)/ 57531(4)	49400(2)/ 49370(2)	534(3)/209(2)
I3	50000 / 50000	0 / 0	50000 / 50000	375(3)/143(2)
I4	80880(2)/81000(2)	−6850(2)/ −7490(2)	51190(2)/ 51240(2)	532(3)/203(2)
S1	8876(2)/ 8913(2)	−578(2)/ −599(1)	1129(2)/ 1135(1)	338(8)/139(6)
S2	7011(2)/ 7012(2)	1467(2)/ 1451(1)	659(2)/ 661(1)	377(9)/148(6)
S3	7225(2)/ 7227(2)	2886(2)/ 2884(1)	2202(2)/ 2206(1)	369(8)/140(6)
S4	9421(2)/ 9464(2)	434(2)/ 425(1)	2808(2)/ 2822(1)	362(8)/142(6)
S5	8314(2)/ 8344(2)	−1920(2)/ −1946(1)	−678(2)/ −678(1)	345(8)/142(6)
S6	6447(2)/ 6443(2)	147(2)/ 129(1)	−1101(2)/ −1098(1)	357(8)/142(6)
S7	8107(2)/ 8123(2)	−3232(2)/ −3264(1)	−2260(2)/ −2265(1)	360(8)/153(6)
S8	5965(2)/ 5966(2)	−720(2)/ −720(1)	−2797(2)/ −2802(1)	342(8)/132(6)
C1	7798(2)/ 7835(6)	58(2)/ 39(5)	377(2)/ 383(3)	30(3)/ 13(2)
C2	8599(2)/ 8640(6)	622(2)/ 615(5)	1865(2)/ 1867(3)	27(3)/ 13(2)
C3	7747(2)/ 7752(6)	1562(2)/ 1559(5)	1643(2)/ 1653(3)	28(3)/ 13(2)
C4	8269(2)/ 8270(7)	2769(2)/ 2743(5)	3151(2)/ 3163(3)	37(4)/ 15(2)
C5	8293(2)/ 8272(7)	1449(2)/ 1421(6)	3372(2)/ 3380(3)	42(4)/ 17(3)
C6	7567(2)/ 7589(6)	−498(2)/ −526(5)	−374(2)/ −371(3)	31(4)/ 13(2)
C7	7630(2)/ 7650(6)	−1929(2)/ −1954(5)	−1670(2)/ −1668(3)	27(3)/ 12(2)
C8	6782(2)/ 6785(6)	−975(2)/ −991(5)	−1865(2)/ −1868(3)	27(3)/ 11(2)
C9	7464(2)/ 7463(6)	−2850(2)/ −2876(5)	−3230(2)/ −3239(3)	36(4)/ 13(2)
C10	5955(2)/ 5940(6)	−2289(2)/ −2293(5)	−3304(2)/ −3310(3)	32(4)/ 14(2)
S11	4153(2)/ 4144(2)	3236(2)/ 3224(1)	9334(2)/ 9335(1)	379(8)/147(6)
S12	5517(2)/ 5515(2)	5457(2)/ 5469(1)	8879(2)/ 8874(1)	374(8)/150(6)
S13	3555(2)/ 3551(2)	1886(2)/ 1855(1)	7764(2)/ 7764(1)	388(8)/157(6)
S14	5164(2)/ 5195(2)	4547(2)/ 4551(1)	7192(2)/ 7182(1)	431(9)/177(6)
C11	4930(2)/ 4909(7)	4726(2)/ 4725(5)	9623(2)/ 9624(3)	32(4)/ 15(3)
C12	4285(2)/ 4286(6)	3237(2)/ 3213(5)	8344(2)/ 8341(3)	29(3)/ 12(2)
C13	4899(2)/ 4911(7)	4254(2)/ 4255(5)	8127(2)/ 8116(3)	30(4)/ 15(2)
C14	4205(2)/ 4221(7)	2063(2)/ 2040(5)	6856(2)/ 6848(3)	34(4)/ 14(2)
C15	3973(2)/ 3981(6)	3338(2)/ 3341(5)	6590(2)/ 6583(3)	36(4)/ 13(2)
S21	8831(2)/ 8790(2)	3348(2)/ 3341(1)	9328(2)/ 9326(1)	366(8)/160(6)
S22	10771(2)/10814(2)	5273(2)/ 5275(1)	8898(2)/ 8897(1)	348(8)/148(6)
S23	8193(2)/ 8172(2)	1961(2)/ 1942(1)	7763(2)/ 7756(1)	351(8)/133(6)
S24	10354(2)/10378(2)	4327(2)/ 4340(1)	7211(2)/ 7201(1)	376(8)/141(6)
C21	9917(2)/ 9918(6)	4714(2)/ 4718(5)	9627(2)/ 9625(3)	30(4)/ 13(2)
C22	9096(2)/ 9068(6)	3251(2)/ 3253(5)	8348(2)/ 8342(3)	28(3)/ 13(2)
C23	9961(2)/ 9973(6)	4133(2)/ 4142(5)	8144(2)/ 8135(3)	29(3)/ 10(2)
C24	8331(2)/ 8337(6)	2335(2)/ 2319(5)	6793(2)/ 6779(3)	36(4)/ 14(2)
C25	9876(2)/ 9887(6)	2788(2)/ 2779(5)	6703(2)/ 6689(3)	35(4)/ 12(2)

[a] Fractional coordinates are × 10^5 for I atoms and × 10^4 for all other atoms. Equivalent U values (in Å^2 units) are × 10^4 for the I and S atoms and × 10^3 for the C atoms. Estimated standard deviations are enclosed in parentheses. $U_{eq} = 1/3\Sigma_i\Sigma_j[U_{ij}\, a_i\, a_j\, a_i^*\, a_j^*]$.

TABLE III

Bond distances (Å) and angles (°) in the ET molecules and I_3-anions of α-$(ET)_2I_3$ at 298/120 K[a]

I1 —I2	2.927(1)/2.930(1)
I3 —I4	2.926(1)/2.930(1)
ET molecule 'A' distances & angles	
S1 —C1	1.738(6)/1.740(6)
S1 —C2	1.763(6)/1.756(6)
S2 —C1	1.734(6)/1.749(6)
S2 —C3	1.743(6)/1.754(6)
S3 —C3	1.740(6)/1.732(6)
S3 —C4	1.809(7)/1.824(6)
S4 —C2	1.737(6)/1.764(6)
S4 —C5	1.821(7)/1.828(6)
S5 —C6	1.744(6)/1.738(6)
S5 —C7	1.750(6)/1.751(6)
S6 —C6	1.729(6)/1.748(6)
S6 —C8	1.757(6)/1.755(6)
S7 —C7	1.737(6)/1.743(6)
S7 —C9	1.805(6)/1.816(6)
S8 —C8	1.746(6)/1.752(6)
S8 —C10	1.820(6)/1.808(6)
C1 —C6	1.376(7)/1.366(7)
C2 —C3	1.355(8)/1.361(8)
C4 —C5	1.539(9)/1.508(8)
C7 —C8	1.346(8)/1.358(7)
C9 —C10	1.528(9)/1.525(8)
C1 —S1 —C2	95.4(3)/ 95.3(3)
C1 —S2 —C3	95.5(3)/ 95.7(3)
C3 —S3 —C4	101.8(3)/101.5(3)
C2 —S4 —C5	99.5(3)/ 99.3(3)
C6 —S5 —C7	95.2(3)/ 95.4(3)
C6 —S6 —C8	95.4(3)/ 95.5(3)
C7 —S7 —C9	102.5(3)/102.4(3)
C8 —S8 —C10	99.8(3)/100.1(3)
C6 —C1 —S1	123.1(5)/123.4(4)
C6 —C1 —S2	121.4(4)/121.2(4)
S1 —C1 —S2	115.5(3)/115.2(3)
C3 —C2 —S1	116.1(4)/117.4(4)
C3 —C2 —S4	127.9(4)/126.6(4)
S1 —C2 —S4	116.0(3)/115.7(3)
C2 —C3 —S3	129.4(4)/130.3(4)
C2 —C3 —S2	117.5(4)/116.2(4)
S2 —C3 —S3	113.0(3)/113.5(3)
C5 —C4 —S3	113.0(4)/113.6(4)
C4 —C5 —S4	111.2(5)/111.5(4)
C1 —C6 —S5	122.9(4)/123.3(4)
C1 —C6 —S6	121.8(4)/121.6(4)
S5 —C6 —S6	115.2(3)/115.0(3)
C8 —C7 —S5	117.2(4)/117.3(4)
C8 —C7 —S7	129.1(4)/128.7(4)
S5 —C7 —S7	113.7(3)/114.0(3)
C7 —C8 —S6	116.7(4)/116.4(4)
C7 —C8 —S8	128.0(4)/128.1(4)
S6 —C8 —S8	115.4(3)/115.6(3)
C10—C9 —S7	113.1(4)/113.9(4)
C9 —C10—S8	112.2(4)/113.2(4)
ET molecule 'B' distances & angles	
S11 —C11	1.726(6)/1.731(6)
S11 —C12	1.751(6)/1.749(6)
S12 —C11	1.746(6)/1.748(6)
S12 —C13	1.760(6)/1.762(6)
S13 —C12	1.740(6)/1.735(6)
S13 —C14	1.798(7)/1.810(6)
S14 —C13	1.753(6)/1.742(6)
S14 —C15	1.826(6)/1.817(6)
C11—C11	1.358(9)/1.358(9)
C12—C13	1.323(8)/1.364(8)
C14—C15	1.513(8)/1.530(8)
C11—S11 —C12	95.8(3)/ 96.1(3)
C11—S12 —C13	95.1(3)/ 96.1(3)
C12—S13 —C14	101.0(3)/101.2(3)
C13—S14 —C15	100.7(3)/100.9(3)
C11—C11—S11	123.9(7)/123.3(6)
C11—C11—S12	121.3(7)/121.9(6)
S11 —C11—S12	114.7(3)/114.6(3)
C13—C12—S13	129.6(4)/128.5(4)
C13—C12—S11	117.3(4)/117.3(4)
S13 —C12—S11	113.1(3)/114.0(3)
C12—C13—S14	128.3(4)/128.8(4)
C12—C13—S12	117.0(4)/115.5(4)
S14 —C13—S12	114.7(3)/115.5(3)
C15—C14—S13	113.9(4)/113.9(4)
C14—C15—S14	112.5(4)/112.4(4)
ET molecule 'C' distances & angles	
S21 —C22	1.743(6)/1.756(6)
S21 —C21	1.752(6)/1.765(6)
S22 —C21	1.750(6)/1.748(6)
S22 —C23	1.766(6)/1.769(6)
S23 —C22	1.747(6)/1.753(6)
S23 —C24	1.799(6)/1.816(6)
S24 —C23	1.758(5)/1.749(5)
S24 —C25	1.814(6)/1.819(6)
C21—C21	1.353(9)/1.360(9)
C22—C23	1.322(8)/1.358(7)
C24—C25	1.529(9)/1.517(8)
C22—S21 —C21	95.6(3)/ 94.7(3)
C21—S22 —C23	94.7(3)/ 95.3(3)
C22—S23 —C24	101.9(3)/101.8(3)
C23—S24 —C25	100.2(3)/100.7(3)
C21—C21—S22	123.5(6)/123.1(6)
C21—C21—S21	121.7(7)/121.5(6)
S22 —C21—S21	114.8(3)/115.3(3)
C23—C22—S23	129.5(4)/128.4(4)
C23—C22—S21	117.2(4)/117.9(4)
S23 —C22—S21	113.3(3)/113.5(3)
C22—C23—S24	128.0(4)/128.1(4)
C22—C23—S22	117.6(4)/116.4(4)
S24 —C23—S22	114.4(3)/115.3(3)
C25—C24—S23	112.9(4)/113.4(4)
C24—C25—S24	112.9(4)/113.0(4)

[a] Estimated standard deviations are enclosed in parentheses.

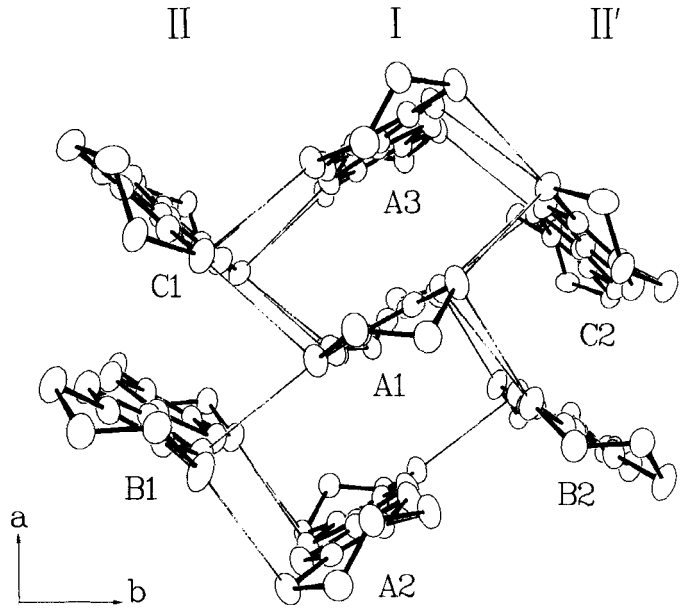

FIGURE 1 The packing motif of ET molecules in the *ab* plane for α-(ET)$_2$I$_3$. The six nearest neighbors to the central ET molecule (which is A1) are labelled A2, A3, B1, B2, C1 and C2. The view is along the normal to the *ab* plane and nearly along the long in-plane molecular axis of each of the three unique ET molecules (A, B and C). The S · · · S contacts less than the van der Waals radii sum (3.6 Å) are indicated by thin lines.

periment, all of the ET molecules in α-(ET)$_2$I$_3$ are chemically equivalent with expected charges of +0.5e. All molecules (and the ethylene groups of the ET molecule) in α-(ET)$_2$I$_3$ are observed to be completely ordered at 298 K and 120 K, in contrast to the positionally disordered C(9)–C(10) ethylene group in β-(ET)$_2$I$_3$.[3]

The comparison of the ET and I_3^- molecular structures in α-(ET)$_2$I$_3$ above and below the MI transition reveals only minor changes. Thus, it is important to investigate whether or not this transition is accompanied by a *significant* change in the overall crystal packing or some other structural feature.

INTERACTION GEOMETRIES AND ENERGIES OF ET-MOLECULE PAIRS

The essence of the 2D packing motif of the ET molecules in α-(ET)$_2$I$_3$ at either 298 K or 120 K is depicted in Figure 1, which shows that there are two different ET stacks (i.e., I and II) per unit cell. Stack I

TABLE IV

Selected interaction parameters for pairs of ET molecules (i–j) in α-$(ET)_2I_3$ at 298/120 K

(i–j) pair	S · · · S contact	distance[a] (Å)	R_{ij} (Å)	ϕ_{ij} (Å)	ΔY_{ij} (Å)	β_{ij} (eV)
A1—A2	S2 · · · S6	3.816/3.744	4.95/4.95	52.1/51.0	0.23/0.25	0.081/0.096
A1—A3	S1 · · · S5	3.928/3.879	4.28/4.18	63.3/63.6	−0.08/−0.09	−0.016/−0.019
A1—B1	S7 · · · S14	3.537/3.467	5.42/5.34	−59.2/−59.8	1.72/1.73	0.026/0.027
A1—B2	S3 · · · S12	3.568/3.540	5.87/5.86	−7.4/−7.6	−1.96/−1.98	0.095/0.109
A1—C1	S6 · · · S23	3.471/3.440	5.32/5.24	−8.6/−9.0	1.80/1.81	0.001/0.002
A1—C2	S8 · · · S23	3.482/3.420	5.69/5.64	−54.1/−54.0	−1.88/−1.90	0.080/0.090
B1—C1	S11 · · · S22	3.877/3.819	4.59/4.54	57.3/56.7	0.07/0.08	−0.019/−0.018

[a] Only the shortest intermolecular S · · · S contact distance is given for each pair of ET molecules. Estimated standard deviations in the distances are ±0.003 Å at 120 K and ±0.002 Å at 298 K.

contains molecules with the geometries of molecule A, and consists of dimeric units (i.e., A1–A2) that repeat along the crystallographic *a* axis. Stack II contains pairs of non-parallel molecules of other geometries (i.e., B and C) that alternate along the *a* axis with uniform spacings. The adjacent ET planes are parallel in stack I, but have a dihedral angle of ~11° in stack II. Due to the arrangement of ET molecules in the unit cell of α-(ET)$_2$I$_3$, there are seven unique pairs (*i*–*j*) of nearest-neighbor ET molecules: (A1–A2), (A1–A3), (A1–B1), (A1–C1), (A1–B2), (A1–C2), (B1–C1), as in Figure 1. In order to analyze the structural changes that accompany the 135 K metal-insulator transition of α-(ET)$_2$I$_3$, we list in Table IV several geometrical parameters that describe the relative arrangement of each (*i*–*j*) pair of ET molecules. Included in Table IV are the shortest S · · · S contact distances in each (*i*–*j*) pair, and the three parameters R_{ij}, ϕ_{ij} and ΔY_{ij}, which describe the relative position of each (*i*–*j*) pair,[22] as shown in Figure 2. Here, $R_{ij} = [(\Delta X)^2 + (\Delta Z)^2]^{1/2}$ and $\phi_{ij} = \tan^{-1}(\Delta Z/\Delta X)$, where the displacement of molecule *j* with respect to *i* is $(\Delta X, \Delta Y, \Delta Z)$ in the Cartesian system defined in **1**. These geometrical parameters show minor changes in crystal packing upon lowering the temperature through the MI transition, which is as expected, since the 2D ET network does not undergo a large structural modification.

Also listed in Table IV are the HOMO interaction energies $\beta_{ij} = \langle\psi_i|H_{\text{eff}}|\psi_j\rangle$ calculated within the extended Hückel method[24] for the (*i*–*j*) pairs of ET molecules. Here ψ_i and ψ_j are the HOMO's of molecules *i* and *j*, respectively, constructed with single-zeta Slater

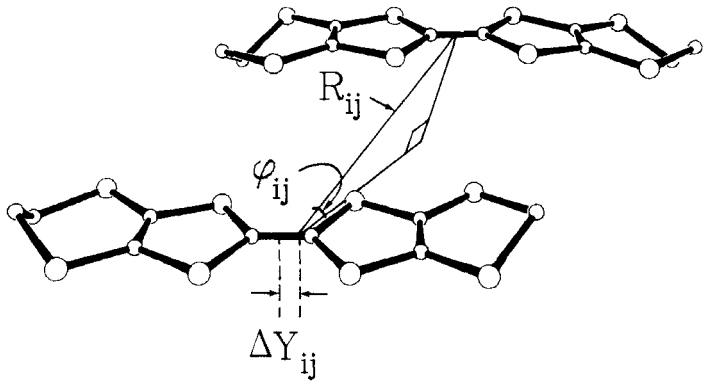

FIGURE 2 The relative orientation of one ET molecule to a neighboring one within a given sheetlike network can be described by the geometrical parameters R_{ij}, ψ_{ij} and ΔY_{ij} (see text).

type atomic orbitals.[25] Upon examination of these HOMO interaction energies, which are mainly responsible for the electrical properties of α-$(ET)_2I_3$ and other $(ET)_2X$ salts,[26] we observe that relatively stronger and weaker interactions alternate along the ET molecular stacks that contain molecules A1, A2 and A3 of Figure 1. As shown in Table IV, the β_{ij} value for the ET molecular pair A1–A2 is approximately 0.09 eV, while β_{ij} for the A1–A3 pair is only -0.02 eV. In summary, of the β_{ij} values of Table IV, there are two sets of interaction energies, those with β_{ij} nearly 0.10 eV (i.e., the stronger interactions) and those with β_{ij} nearly 0.01 eV (i.e., the weaker interactions). As schematically illustrated in Figure 3, the inter-cation motif that is obtained for α-$(ET)_2I_3$ is a zigzag array of relatively stronger interactions (connecting lines in Figure 3) that do not propagate directly along the stacking (*a* axis) or interstack (*b* axis) direc-

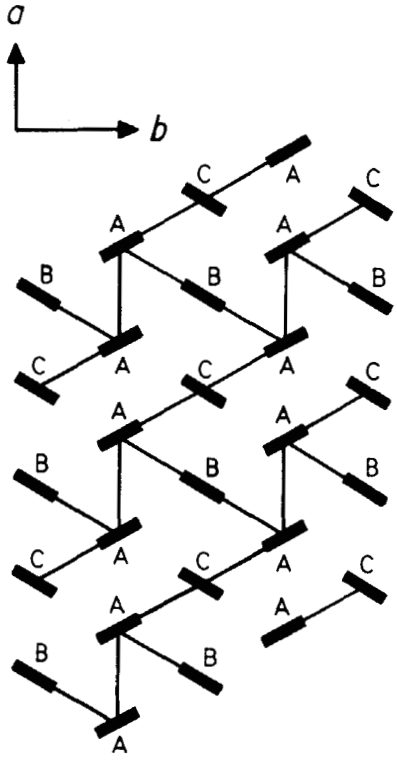

FIGURE 3 A schematic illustration of the connectivity (thin lines) of the interactions between pairs of ET molecules in α-$(ET)_2I_3$ that have β_{ij} values of ~0.10 eV (see Table IV), which zigzag throughout the *ab* plane.

tions of the ET molecular network. As expected from the constancy of the geometrical parameters R_{ij}, ϕ_{ij}, ΔY_{ij} and the S · · · S contacts in Table IV, the β_{ij} values also do not display any large differences upon lowering the temperature. The β_{ij} values calculated by using the double-zeta Slater type atomic orbitals,[27] which are not included in Table IV for simplicity, reveal the same trends as described above for the single-zeta basis calculations.

INTERMOLECULAR CONTACTS WITH THE I_3^- ANIONS

In order to conclude the description of the 298 K and 120 K crystal structures of α-(ET)$_2$I$_3$, let us examine the packing of the I_3^- anions in their layers which separate the 2D ET networks. Figure 4 is a stereoview of an ET network and an adjacent I_3^- layer, and shows that the I_3^- anions form two unique chains along the *a* axis, with two sets of I · · · I contacts as listed in Table V. The lengths of these two I · · · I contacts, which are typical values for polyiodides,[28] are ~0.42 Å shorter than the van der Waals radii[29] sum for two iodide ions (4.30 Å) at room temperature and contract by unequal amounts (0.05 Å versus 0.01 Å) upon temperature lowering to 120 K. This situation parallels that of the pairwise separations within the ET network, which also contract by unequal amounts (compare the R_{ij} values for A1–A2 vs. A1–A3, A1–B1 vs. A1–B2 and A1–C1 vs. A1–C2 in Table IV). As expected from the 0.05 Å contraction of the *c* axis upon lowering the temperature from 298 K to 120 K (see Table I), the ET-anion contacts along this direction, namely I · · · S and I · · · H, contract by amounts within the range 0.01–0.07 Å. Table V lists the I · · · S and

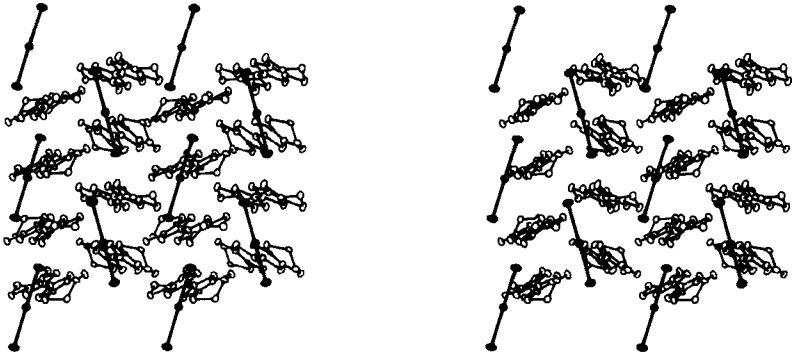

FIGURE 4 A stereoview of the packing arrangement between an ET network and an adjacent layer of I_3^- anions in α-(ET)$_2$I$_3$ viewed along the crystallographic c^* axis.

TABLE V

Interaction distances in α-$(ET)_2I_3$ at 298/120 K

A. Anion-Anion I · · · I contact distances less than the van der Waals radii sum of 4.30 Å.[a]

Contact	298/120 K value
I2 · · · I2′	3.882(1)/3.833(1)
I4 · · · I4′	3.885(1)/3.874(1)

B. All I · · · S and I · · · H distances less than the respective van der Waals radii sums of 4.00 Å and 3.35 Å.[a]

Contact	298/120 K value	Contact[b]	298/120 K value
I4 · · · S4	3.976(2)/3.914(2)	I2 · · · H4A	2.85 / 2.83
I1 · · · S24	3.976(2)/3.944(2)	I4 · · · H14A	2.90 / 2.89
I3 · · · S8	3.991(2)/3.973(2)	I2 · · · H9A	2.93 / 2.91
		I4 · · · H24B	3.02 / 3.03
		I3 · · · H14A	3.13 / 3.09
		I2 · · · H24A	3.22 / 3.16
		I1 · · · H25B	3.23 / 3.17
		I4 · · · H9B	3.23 / 3.16
		I1 · · · H4A	3.27 / 3.26
		I3 · · · H10A	3.28 / 3.23

[a] The van der Waals radii[29] used here are: 2.15 Å for I; 1.85 Å for S; and 1.2 Å for H.

[b] The H atom positions were calculated using 1.09 Å C—H distances.

I · · · H contact distances that are less than their respective van der Waals radii[29] of 4.00 Å and 3.35 Å, respectively, at both temperatures. There are many I · · · H contacts with distances less than 3.35 Å (see Table V), and each terminal I atom of both I_3^- anions has two I · · · H contact distances in the range 2.9–3.0 Å. Since these I · · · H distances are very short compared to the van der Waals radii[29] sum and they do not contract by a significant amount as the temperature is decreased from 298 K to 120 K, there is likely a significant ET-anion interaction via these I · · · H contacts even at room temperature. Future neutron diffraction studies of α-$(ET)_2I_3$ will be very useful in ascertaining the precise H atom positions that are necessary to accurately describe the ET-anion interaction.

BAND ELECTRONIC STRUCTURE

To probe the nature of the 135 K MI transition of α-$(ET)_2I_3$, we have carried out tight-binding band electronic structure calculations[26] for

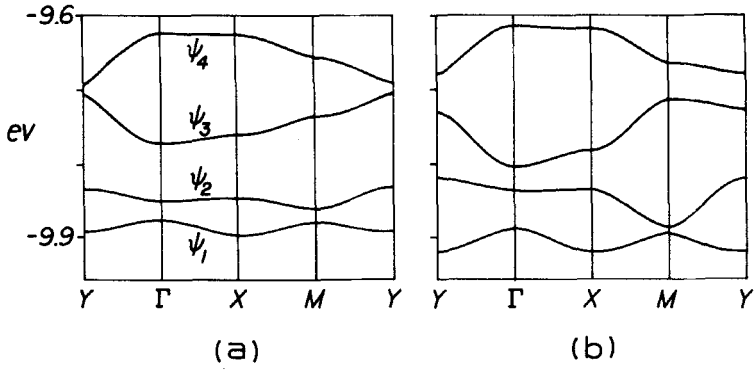

FIGURE 5 Electron energy dispersion relations for the four bands derived largely from the HOMO's of the ET molecules of α-(ET)$_2$I$_3$ (A) at 298 K and (B) at 120 K, using single-zeta Slater type orbital basis. The boundary points of the first Brillouin zone are: ($a^*/2$, 0, 0) for X, (0, $b^*/2$, 0) for Y, ($a^*/2$, $b^*/2$, 0) for M and (0, 0, 0) for Γ.

the 2D ET networks determined at 298 K and 120 K. Our calculations employed both single- and double-zeta Slater type atomic orbitals.[25,27] Since α-(ET)$_2$I$_3$ has four ET molecules per unit cell (i.e., molecules A1, A2, B1 and C1 in Figure 1), there occur four bands derived mainly from the HOMO's of these four ET molecules. Figures 5 and 6 show the dispersion relations of these four bands at 298 and 120 K calculated with single- and double-zeta basis sets, respectively. Due to the formal oxidation of $(ET)_2^+$, there are six electrons that remain per unit cell to fill the four bands. The essential features of the band

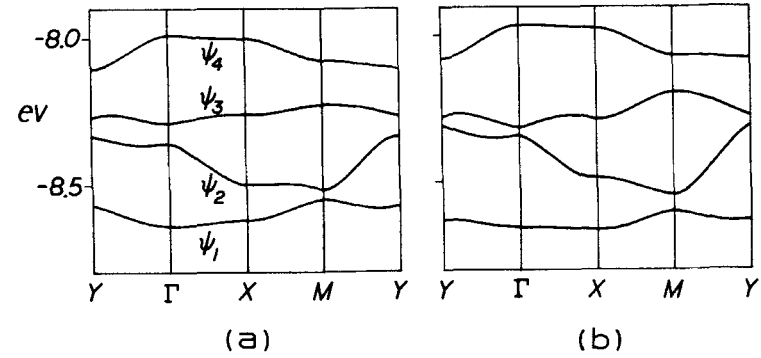

FIGURE 6 Electron energy dispersion relations for the four bands derived largely from the HOMO's of the ET molecules of α-(ET)$_2$I$_3$ (A) at 298 K and (B) at 120 K using double-zeta Slater type orbital basis. The boundary points of the first Brillouin zone are the same as shown in Figure 5.

electronic structures of α-$(ET)_2I_3$ shown in Figures 5 and 6 can be summarized as follows:

(i) At both temperatures, the four bands span a very narrow energy range (i.e., ~0.3 eV and ~0.7 eV for the single- and double-zeta basis sets, respectively).

(ii) At both temperatures, each individual band is separated from the others in all directions and is narrow in bandwidth (less than 100 meV).

(iii) The upper two bands, ψ_3 and ψ_4, display maximum dispersion along $\Gamma \rightarrow Y$ and $X \rightarrow M$, which are directions parallel to the crystallographic b^* and $(a^* + b^*)$ axes, respectively. Thus, the strongest interactions are *between*, rather than within, the ET molecular stacks.)

(iv) The single-zeta basis calculations show that the ψ_3 and ψ_4 bands are separated by a small direct band gap of 13 meV at 298 K, and at 120 K by a larger indirect band gap of 35 meV (between Brillouin zone boundaries M and Y). On the other hand, the double-zeta basis calculations show that the ψ_3 and ψ_4 bands have indirect band gaps that are greater than 100 meV at both temperatures.

Electron localization usually occurs for systems with narrow bands[30] such as those shown in Figures 5 and 6. If electron localization does not occur for α-$(ET)_2I_3$, the single-zeta basis calculations summarized in Figure 5 suggest that this compound is a semiconductor with a very small band gap above T_{MI}, but with a larger band gap below T_{MI}. Within this picture, the apparent metallic behavior of α-$(ET)_2I_3$ above 135 K arises from thermal excitation of electrons across the very small gap, which makes the two bands, ψ_3 and ψ_4, partially filled. In this case, Figure 5A indicates that the ψ_3 band is partially filled and the ψ_4 band is partially empty for wavevectors in the vicinity of Y, leading to closed Fermi surfaces for these two bands, as schematically shown in Figure 7. This model is consistent with the reported 2D metallic behavior of α-$(ET)_2I_3$.[17,18] Below 135 K, the presence of a larger band gap would be responsible for normal (not activated) semiconductor behavior for α-$(ET)_2I_3$. Such a simple interpretation can not be obtained from the results of the double-zeta basis calculations summarized in Figure 6.

Within the one-electron picture, the above interpretation of the MI transition based upon Figure 5 seems reasonable. But this explanation is valid under the assumption that electron localization does not occur in α-$(ET)_2I_3$. However, since each of the four bands in either Figure 5 or 6 is very narrow and since each adjacent pair of bands has a small energy gap, it is probable that electron localization

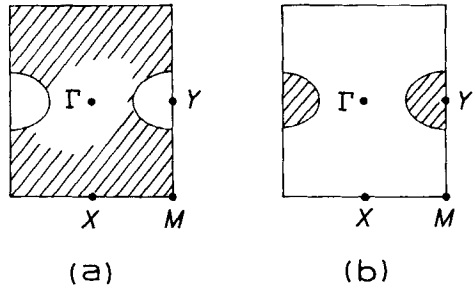

FIGURE 7 The Fermi surfaces that are expected from the dispersion relations in Figure 5: (A) the hole-like Fermi surface of the ψ_3 band; (B) the electron-like Fermi surface of the ψ_4 band. The sizes of both Fermi surfaces shown are arbitrary, and depend on the extent of thermal excitation across the band gap.

does occur in α-(ET)$_2$I$_3$. Then the one-electron band picture presented above may have to be modified significantly by accounting for either electron-electron repulsion or mixed valence of ET molecules (e.g., $A^+A^+B^0C^0$, $A^+A^0B^+C^0$, etc. with respect to Figure 1). To ascertain whether or not the ET molecules are in mixed- or mono-valence states, x-ray photoelectron spectroscopic studies on α-(ET)$_2$I$_3$ would be extremely valuable.

CONCLUSIONS

The results of the crystal structure determinations carried out above (298 K) and below (120 K) the 135 K MI transition in α-(ET)$_2$I$_3$ show that there are minor changes in the crystal packing based on geometrical parameters R_{ij}, ϕ_{ij} and ΔY_{ij}, and minor changes in the relative strengths of the interactions between neighboring ET molecules based on interaction energies, β_{ij}. However, there are noticeable differences in the band structures calculated above and below the MI transition. Both the single- and double-zeta basis calculations indicate that α-(ET)$_2$I$_3$ is not a semi-metal, but a *semiconductor* above and below T_{MI}. In addition, the single-zeta basis results suggest that the metallic behavior of α-(ET)$_2$I$_3$ above T_{MI} originates from the very small band gap. However, the valence and conduction bands of α-(ET)$_2$I$_3$ are calculated to be very narrow, and are separated by a small band gap on the basis of either single- or double-zeta orbitals. Therefore, electron localization in α-(ET)$_2$I$_3$ is quite probable and the explanation for the 135 K MI transition might require a theoretical approach beyond the one-electron theory.

Acknowledgment

Research at Argonne National Laboratory is sponsored by the U.S. Department of Energy (DOE), Office of Basic Energy Sciences, Division of Materials Sciences under contract W-31-109-Eng-38. This work is in part supported by the Camille and Henry Dreyfus Foundation through a Teacher-Scholar Award to M.-H. Whangbo. The authors express their appreciation for computing time on the ER-cray computer, made available by the DOE.

Supplementary Material

Tables of refined anisotropic thermal parameters for all non-hydrogen atoms, least-squares planes through the ET molecules, the calculated H-atom positions and lists of observed and calculated structure factors for α-$(ET)_2I_3$ at 298 K and 120 K (87 pages). This material may be obtained by contacting Gordon and Breach, One Park Avenue, New York, NY 10016.

References

1. E. B. Yagubskii, I. F. Shchegolev, V. N. Laukhin, P. A. Kononovich, M. V. Kartsovnik, A. V. Zvarykina and L. I. Buravov, *Pis'ma Zh. Eksp. Teor. Fiz.*, **39**, 12 (1984); *JETP Lett.* (Engl. Transl.) **39**, 12 (1984).
2. a. G. W. Crabtree, K. D. Carlson, L. N. Hall, P. T. Copps, H. H. Wang, T. J. Emge, M. A. Beno and J. M. Williams, *Phys. Rev.*, **B30**, 2958 (1984); b. K. D. Carlson, G. W. Crabtree, L. N. Hall, T. P. Copps, H. H. Wang, T. J. Emge, M. A. Beno and J. M. Williams, *Mol. Cryst. Liq. Cryst.*, **119**, 357 (1985).
3. J. M. Williams, T. J. Emge, H. H. Wang, M. A. Beno, T. P. Copps, L. N. Hall, K. D. Carlson and G. W. Crabtree, *Inorg. Chem.*, **23**, 2558 (1984).
4. J. M. Williams, H. H. Wang, M. A. Beno, T. J. Emge, L. M. Sowa, T. P. Copps, F. Behroozi, J. N. Hall, K. D. Carlson and G. W. Crabtree, *Inorg. Chem.*, **23**, 3839 (1984).
5. K. D. Carlson, G. W. Crabtree, L. N. Hall, F. Behroozi, P. T. Copps, L. M. Sowa, L. Nuñez, M. A. Firestone, H. H. Wang, M. A. Beno, T. J. Emge and J. M. Williams, *Mol. Cryst. Liq. Cryst.*, **125**, 159 (1985).
6. H. H. Wang, M. A. Beno, U. Geiser, M. A. Firestone, K. S. Webb, L. Nuñez, G. W. Crabtree, K. D. Carlson, J. M. Williams, L. J. Azevedo, J. F. Kwak and J. E. Schirber, *Inorg. Chem.*, **24**, 2465 (1985).
7. K. D. Carlson, G. W. Crabtree, L. Nünez, H. H. Wang, M. A. Beno, U. Geiser, M. A. Firestone, K. S. Webb and J. M. Williams, *Solid State Commun.*, **57**, 89 (1986).
8. M. Tokumoto, H. Anzai, H. Bando, G. Saito, N. Kinoshita, K. Kajimura and T. Ishiguro, *J. Phys. Soc. Jpn.*, **54**, 869 (1985).
9. R. P. Shibaeva, V. F. Kaminskii and E. B. Yagubskii, *Mol. Cryst. Liq. Cryst.*, **119**, 361 (1985).
10. V. F. Kaminskii, T. G. Prokhorova, R. P. Shibaeva and E. B. Yagubskii, *Pis'ma Zh. Eksp. Teor. Fiz.*, **39**, 15 (1984); *JETP Lett.* (Engl. Transl.) **39**, 15 (1984).
11. a. T. J. Emge, H. H. Wang, M. A. Beno, P. C. W. Leung, M. A. Firestone, H. C. Jenkins, J. D. Cook, K. D. Carlson, J. M. Williams, E. L. Venturini, L. J. Azevedo and J. E. Schirber, *Inorg. Chem.*, **24**, 1736 (1985); b. T. J. Emge, P. C. W. Leung, M. A. Beno, H. H. Wang, M. A. Firestone, K. S. Webb, K. D. Carlson, J. M. Williams, E. L. Venturini, L. J. Azevedo and J. E. Schirber, *Mol. Cryst. Liq. Cryst.*, **132**, 363 (1986).

12. P. C. W. Leung, M. A. Beno, T. J. Emge, H. H. Wang, M. K. Bowman, M. A. Firestone, L. M. Sowa and J. M. Williams, *Mol. Cryst. Liq. Cryst.*, **125**, 113 (1985).
13. The structure of α-(ET)$_2$I$_3$ (triclinic phase): K. Bender, K. Dietz, H. Endres, H. W. Helberg, I. Henning, H. J. Keller, H. W. Schäfer and D. Schweitzer, *Mol. Liq. Cryst.*, **107**, 45 (1984).
14. The structures of the isostructural α-(ET)$_2$IBr$_2$ and α-(ET)$_2$IBrCl: M. A. Beno, T. J. Emge, M. A. Firestone, L. M. Sowa, H. H. Wang, J. M. Williams and M.-H. Whangbo, to be published.
15. The structures of the isotstructural salts, α′-(ET)$_2$Au(CN)$_2$, α′-(ET)$_2$Ag(CN)$_2$ and α′-(ET)$_2$AuBr$_2$: M. A. Beno, M. A. Firestone, P. C. W. Leung, L. M. Sowa, H. H. Wang, J. M. Williams and M.-H. Whangbo, *Solid State Commun.*, **57**, 735 (1986).
16. K. Bender, I. Hennig, D. Schweitzer, K. Dietz, H. Endres and H. J. Keller, *Mol. Cryst. Liq. Cryst.*, **108**, 359 (1984).
17. H. Schwenk, F. Gross, C.-P. Heidmann, K. Andres, D. Schweitzer and H. Keller, *Mol. Cryst. Liq. Cryst.*, **119**, 329 (1985).
18. B. Koch, H. P. Geserich, W. Ruppel, D. Schweitzer, K. H. Dietz and H. J. Keller, *Mol. Cryst. Liq. Cryst.*, **119**, 343 (1985).
19. E. L. Venturini, L. J. Azevedo, J. E. Schirber, J. M. Williams and H. H. Wang, *Phys. Rev.*, **B32**, 2819 (1985).
20. H. Kobayashi, A. Kobayashi, Y. Sasaki, G. Saito and H. Inokuchi, *Chem. Lett.*, 183 (1984).
21. T. Mori, A. Kobayashi, Y. Sasaki, H. Kobayashi, G. Saito and H. Inokuchi, *Chem. Lett.*, 957 (1984).
22. T. Mori, A. Kobayashi, Y. Sasaki, H. Kobayashi, G. Saito and H. Inokuchi, *Bull. Chem. Soc. Jpn.*, **57**, 627 (1984).
23. The neutron data was collected at the IPNS facility at Argonne National Laboratory by means of a time-of-flight Laue technique that employed a position-sensitive area detector; A. J. Schultz, P. C. W. Leung, T. J. Emge and J. M. Williams, unpublished results.
24. a. R. Hoffmann, *J. Chem. Phys.*, **39**, 1397 (1963); b. A modified Wolfsberg-Helmholz formula [J. H. Ammeter, H.-B. Bürgi, J. C. Thibeault and R. Hoffmann, *J. Am. Chem. Soc.*, **100**, 3686 (1978)] was used to calculate $H_{\mu\nu}$ (see reference 30 and 31).
25. For S, C and H atoms, the orbital exponent ζ_μ and the valence shell ionization potential $H_{\mu\nu}$ of each single-zeta atomic orbital employed in our calculations are as follows: 1.817, −20.0 eV for S 3*s*; 1.817, −13.3 eV for S 3*p*; 1.625, −21.4 eV for C 2*s*; 1.625, −11.4 eV for C 2*p*; 1.30, −13.6 eV for H 1*s*.
26. a. M.-H. Whangbo, J. M. Williams, P. C. W. Leung, M. A. Beno, T. J. Emge, H. H. Wang, K. D. Carlson and G. W. Crabtree, *J. Am. Chem. Soc.*, **107**, 5815 (1985); b. M.-H. Whangbo, J. M. Williams, P. C. W. Leung, M. A. Beno, T. J. Emge and H. H. Wang, *Inorg. Chem.*, **24**, 3500 (1985).
27. For S and C atoms, each atomic orbital was represented by a linear combination of two Slater type orbitals of exponents ζ_μ and ζ'_μ with the weighting coefficients c_μ and c'_μ, respectively [E. Clementi, C. Roetti, *At. Data Nucl. Data Tables*, **14**, 177 (1974)]. The ζ_μ, ζ'_μ, c_μ and c'_μ values employed in our calculations are, respectively: 2.662, 1.688, 0.5564, 0.4874 S 3*s*; 2.338, 1.333, 0.5212, 0.5443 for S 3*p*; 1.831, 1.153, 0.7616, 0.2630 for C 2*s*; and 2.730, 1.257, 0.2595, 0.8025 for C 2*p*.
28. a. P. Coppens, "*Extended Linear Chain Compounds*," J. S. Miller, ed., Plenum, New York, pp. 333–356 (1980); b. F. H. Herbstein, M. Kapon, *Philos. Trans. Royal Soc. London* **291**, 199 (1979).
29. a. L. Pauling, "*The Nature of the Chemical Bond*," Cornell University Press: Ithaca, New York (1960); b. A. Bondi, *J. Phys. Chem.*, **68**, 441 (1964).
30. a. N. F. Mott, "*Metal-Insulator Transitions*," Barnes and Noble: New York,

New York (1977); b. B. H. Brandow, *Adv. Phys.*, **26**, 651 (1977); c. P. W. Anderson, *Solid State Phys.*, **14**, 99 (1963); d. J. Hubbard, *Proc. R. Soc. London A*, **276**, 238 (1963); e. J. Kanamori, *Prog. Theor. Phys.*, **30**, 275 (1963); f. M.-H. Whangbo, *J. Chem. Phys.*, **75**, 4983 (1981); g. M.-H. Whangbo, *J. Chem. Phys.*, **73**, 3854 (1980); h. M.-H. Whangbo, *J. Chem. Phys.*, **70**, 4963 (1979).